

Published in final edited form as:

Nat Photonics. 2013 February 1; 7(2): 93–101. doi:10.1038/nphoton.2012.361.

Advances in multiphoton microscopy technology

Erich E. Hoover^{1,2,*} and Jeff A. Squier^{1,2,*}

¹Center for Microintegrated Optics for Advanced Bioimaging and Control, Colorado School of Mines, 1523 Illinois Street, Golden, Colorado 80401, USA.

²Department of Physics, Colorado School of Mines, 1523 Illinois Street, Golden, Colorado 80401, USA.

Abstract

Multiphoton microscopy has enabled unprecedented dynamic exploration in living organisms. A significant challenge in biological research is the dynamic imaging of features deep within living organisms, which permits the real-time analysis of cellular structure and function. To make progress in our understanding of biological machinery, optical microscopes must be capable of rapid, targeted access deep within samples at high resolution. In this Review, we discuss the basic architecture of a multiphoton microscope capable of such analysis and summarize the state-of-the-art technologies for the quantitative imaging of biological phenomena.

New windows in biological exploration are being opened through the continuing development of novel optical multiphoton microscopy (MPM) techniques. In this imaging paradigm, near-infrared (near-IR) femtosecond lasers are used to excite optical processes that can be accessed only through the application of two (or more) photons. Two-photon excitation fluorescence (TPEF) — a process driven by the simultaneous absorption of two near-infrared photons by a single fluorophore — is one example of such a technique¹. The probability of triggering a multiphoton process, such as TPEF, is extremely unlikely to occur. Interactions are therefore restricted to the focal plane of the objective, where the beam intensity is maximized, which provides the optical sectioning necessary for the non-perturbative analysis of living systems.

Since its inception, MPM has permitted a variety of unique explorations into highly scattering materials. These studies have examined membrane potentials on the single-molecule scale², the non-invasive observation of embryo development³ and the simultaneous multiplane imaging of calcium transportation in transgenic mice⁴. The ability to perform such explorations is a direct result of the inherent optical sectioning of multiphoton microscopes^{1,5} and the reduction in photobleaching outside of the imaging plane^{1,5–7}. Multiphoton microscopes also benefit from the ability to utilize longer excitation wavelengths (700 nm and greater) than confocal techniques, thus making them less biologically harmful^{6,7} and more penetrating in scattering tissue^{7–11}. In addition, multiphoton microscopes can frequently take advantage of the endogenous contrast mechanisms inherent to many samples, thus permitting the exploration of untreated specimens^{3,12–15}.

As shown in Fig. 1, a typical multiphoton microscope is composed of a femtosecond laser, a scanning system, a low-magnification high-numerical-aperture (NA) microscope objective, a wavelength-sensitive dichroic and a single-element detector. The scanning system is an intermediate optical system that is used to raster the excitation beam in a two-dimensional (2D) field at the full NA of the objective. The objective is generally used both for excitation and to collect the signal photons. These signal photons are separated from the excitation beam on the return path using a wavelength-sensitive dichroic. Finally, the separated signal is collected by a single-element detector such as a photomultiplier tube (PMT).

This scanning behaviour and point-by-point detection is a defining characteristic of most MPM systems, and differs significantly from more traditional ‘whole-field’ microscopy platforms, which generally use a 2D detector such as a CCD camera to collect data from the entire imaging plane simultaneously. This important distinction allows multiphoton microscopes to perform efficient, deep explorations within scattering tissues^{10,16} by including data from multiply scattered signal photons, which might otherwise introduce a background fog^{7,9}. Whole-field detection comes at the cost of confining imaging to within a few tens of micrometres of the surface of a scattering sample; this trade-off is an important consideration when exploring biological behaviour in scattering media.

The multiphoton microscope design discussed here allows MPM to address one of the toughest challenges since the inception of optical microscopy: achieving image contrast at the cellular level in thick, scattering specimens. By their very nature, cells are quite thin (a few micrometres); such small path lengths provide little absorption, path length differences or scattering — all of which can provide a detailed view of the intricacies of the biological machinery. The use of a femtosecond laser as the light source for the microscope has enabled the generation of an entirely new class of contrast mechanisms within such specimens. Remarkably, these lasers provide intensities of the order of tens of gigawatts per square centimetre with modest focusing (for example, 0.65 NA) and relatively low average powers (milliwatts). At such intensities, the electric field at the focus creates a separation of positive and negative charges, thus momentarily polarizing the material. In fact, the induced time-varying polarization is significantly overdriven, resulting in the generation of new optical signals — distinctive from the excitation beam — that can be used to visualize structure and function in an unprecedented fashion. Substantive reviews of the broad array of nonlinear processes now used in imaging can be found in studies by Yue *et al.*¹⁷ and Chung *et al.*¹⁸.

Today, this nonlinear polarization can be generated with pulses as short as 10 fs, which represents a pulse consisting of only five or six optical cycles^{19–21}. This result is remarkable given the complexity of the optical system that is necessary to deliver such broadband light to the specimen. Combining scan optics with well-corrected high-NA optics poses significant challenges for producing a focal spot that is both diffraction-limited in space and transform-limited in time. Whether a pulse of 100 fs or 10 fs is used as the excitation source, it is desirable to achieve these space–time limits in order to optimize the detected optical signals and get the most out of each pixel.

In addition to maximizing information content, deep imaging is also of great interest to the biological community. As a result, a variety of approaches have been developed to help multiphoton microscopes overcome depth limitations. In this Review, we discuss a number of strategies and design constraints for imaging at depth.

Finally, we survey a number of technologies that can be used to increase the frame rate of a multiphoton microscope, and thus its ability to measure dynamics. From this perspective, the most significant issue is photon scarcity at high imaging rates (>30 Hz for a 2D image —

less than 1 μs per pixel), as the number of laser pulses per pixel dwell time and the excitation efficiency of the nonlinearity of interest become critical issues that dictate image contrast.

After taking into account these disparate issues involved in generating image contrast, MPM provides a set of dynamic tools for addressing a variety of problems. This Review will help facilitate an understanding of the strengths and limitations of many of the common MPM techniques, thus allowing the reader to utilize MPM to its full potential for addressing a variety of real-world imaging tasks. The range of technology being developed in this field is truly impressive and, as such, the scope of this Review is limited. More than ever, it is important to consult the literature when developing a multiphoton microscope for specific applications^{7,22–26}.

Getting the most out of each pixel

There is an incredible amount of information available at the focus of a multiphoton microscope; however, optimizing image content is only possible by paying careful attention to the production of a well-focused pulse in terms of both the spatial wavefront and the temporal pulsefront. This attention is crucial because the production of a well-focused pulse ensures the highest possible intensity at the focus, thereby maximizing the multiphoton signal generation. The quality of this focus is reduced by linear dispersion from the refractive optics in the microscope resulting from: first, an increase in the pulse duration; and, second, asymmetric distortion of the pulse in time^{25,26}. Most of these effects can effectively be pre-compensated through any number of means, including prism pairs, dispersion-compensating mirrors and active pulse-shaping schemes. Work on improving compensation to enable the production of extremely short pulses (10 fs and less) is particularly exciting. As stated earlier, with careful attention to the net dispersion of the microscope, pulsewidths of less than 10 fs can be produced at the focus^{19–21}. Invariably, as the pulse duration limits are advanced, researchers also push the boundaries for new discoveries, from both an imaging perspective and a basic light–matter interaction perspective. Additionally, there is a pragmatic side to extending this limit, as the extreme bandwidth of short pulses (>100 nm) requires a highly achromatic imaging system. Designing for this constraint also benefits users who operate at longer pulse durations (100 fs) but desire an efficient tunable microscope over tens or even hundreds of nanometres. Furthermore, higher-order dispersion compensation, even at these modest pulsewidths, can have a quantifiable increase in the detected photon yield²⁷.

Once diffraction-limited focal conditions are achieved, a remarkable number of multiphoton processes become accessible. An enormous amount of information can be obtained from each image pixel simultaneously, which typically encompasses a femtolitre volume of the specimen. The most commonly exploited nonlinear processes so far include absorptive mechanisms, such as TPEF¹, and parametric processes, such as second-harmonic generation (SHG)²⁸, third-harmonic generation¹², sum-frequency generation^{15,29}, stimulated Raman scattering³⁰ and coherent anti-Stokes Raman scattering^{17,31}. Used in combination, these techniques provide information about a microscopic environment in terms of the chemical, structural and operative mechanisms within living systems.

Multimodal imaging

Lasers capable of simultaneously and efficiently exciting a broad range of these nonlinearities are not prohibitively complex, as demonstrated by Chen *et al.*³². Their system incorporates a femtosecond laser that pumps an optical parametric oscillator in tandem. The fundamental beam from the Ti:sapphire oscillator is tuned to 790 nm and used to drive the optical parametric oscillator, as well as provide an excitation source for TPEF and SHG

imaging. The optical parametric oscillator signal (1,290 nm) and idler (2,036 nm) beams perform several functions. The 1,290 nm beam can be used for both SHG and third-harmonic generation imaging, whereas the frequency-doubled idler beam (1,018 nm) is used as the Stokes wavelength in conjunction with the main laser wavelength (790 nm) to provide a pump for coherent anti-Stokes Raman scattering, which is tuned to the vibrational CH₂ stretch suitable for lipid detection.

Figure 2 is an image of a blood vessel in kidney tissue — an excellent example of a multimodal image that combines the aforementioned contrast mechanisms. In this case, the SHG signal (blue) delineates collagen, the TPEF signal (green) marks the elastin of the vascular wall in addition to intracellular nicotinamide adenine dinucleotide (NADH), and the coherent anti-Stokes Raman scattering signal (red) shows lipids in adipose cells. The image was taken at 0.75 NA, with a pixel dwell time of 4 μ s and a field-of-view measuring 300 μ m \times 300 μ m.

Fluorescence lifetime

Remarkably, even considering this broad array of contrast mechanisms, there is still more information to be had from each pixel of a multiphoton image. The environment can often be further explored, for example, by measuring fluorophore lifetimes. Additionally, lifetime measurements can provide a mechanism for discriminating between different fluorescent labels that may have spectrally similar signatures. Fluorescent lifetime imaging lends itself quite naturally to TPEF imaging as a result of the three-dimensional (3D) confinement of the excitation. Time-correlated single-photon counting is one of the most mature technologies for performing lifetime measurements, and it is extremely well-suited to today's multiphoton imaging platforms^{33,34}. In this approach, the lifetime of a sample is given by a histogram built from the arrival times of individual signal photons collected by a fast detector (for example, a PMT), which makes it suitable for use even within scattering specimens.

Figure 3 is an example of using lifetime measurements to discriminate between spectrally similar fluorophores³⁵. In this case, cells labelled with propidium iodide and vessels labelled with Texas Red dextran are indistinguishable when measuring the intensity of the TPEF signal alone. This situation is particularly evident in Fig. 3a. However, if the image is reformulated based on the fluorescence lifetime (Fig. 3b), contrast between the labels becomes evident. A final image based on fluorescent lifetime and photon counts renders a composite image (Fig. 3c) that enables the unambiguous determination of the fluorophore and its targeted structure.

Pulse shaping

Fluorophores can also be selectively excited or distinguished by altering the shape of the excitation pulse^{36–38}. The basis for many efforts to use pulse shape as a contrast mechanism is the formative work of Meshulach and Silberberg³⁹. For example, by controlling the third-order spectral phase of a broadband excitation pulse, Pillai *et al.*⁴⁰ demonstrated selective TPEF imaging in living *Drosophila* embryos. In this approach, phase-only control enables selective excitation of either endogenous fluorescence or enhanced green fluorescence protein (eGFP)-labelled bodies, and altering the pulse shape at kilohertz rates readily enables dynamic imaging.

New classes of contrast mechanisms can also be exploited if one alters the pulse amplitude, rather than relying solely on phase control. For example, by reshaping the pulse such that a high-intensity fast component resides on a slower low-intensity background component, with each component consisting of equal areas, it becomes possible to measure the amount of two-photon absorption or self-phase modulation that is accumulated by the pulse at the

focal plane^{41–43}. This pulse shape is created by effectively masking out the central frequency of the pulse in the spectral domain (that is, digging a hole at the central wavelength in the pulse spectrum). At the focus, this spectral hole is refilled through two-photon absorption processes or self-phase modulation. Fortunately, these two mechanisms can be distinguished as the field at the replenished frequency is 90° out of phase for two-photon absorption, with respect to self-phase modulation. Significantly, endogenous molecular tags such as melanin or haemoglobin⁴¹, which are nominally transparent, can be distinguished by using two-photon absorption as the contrast agent, whereas neuronal activity can be tracked using self-phase modulation⁴³.

Imaging deep

One task that compounds the challenge of generating image contrast in a thin specimen (such as a cell) is the task of imaging cells and cellular function while embedded deep (hundreds of micrometres) within an organism. Switching to the longer wavelengths necessary to promote efficient multiphoton excitation and detection (near-infrared, 750–1,100 nm) can increase image depths by a factor of two or three in multiphoton systems, when compared with their traditional confocal counterparts. These wavelengths are intrinsically more penetrating owing to their increased scattering length, with the maximum wavelength being limited by the absorption properties of the materials in the specimen. In neuronal tissue — a common MPM application — this limit is set by the blood and water in the brain and therefore limits the excitation wavelength to around 1,300 nm (ref. 10). However, it is important to note that the two-photon cross-section for any fluorophore is spectrally dependent and can therefore also limit the excitation wavelength when performing TPEF.

High-energy lasers

Different strategies can be employed to push the maximum imaging depth, which has now exceeded 1 mm. To maintain sufficient intensity at the focus when reaching significant depths in scattering media, one of the primary tactics is to increase the energy of the excitation pulse^{44–46}. For example, using ~150 fs pulses, amplified to the microjoule level (at a repetition rate of 200 kHz) and centred at a wavelength of 953 nm, Theer *et al.*¹⁶ used TPEF to image GFP-labelled neurons at depths of up to a millimetre within a sample. This strategy functions as a result of the signal dependence on unscattered (or ballistic) excitation light. As the focus is pushed deeper into the specimen, the excitation beam is depleted of these ballistic photons, primarily as a result of scattering, and the excitation efficiency is subsequently reduced. Increasing the pulse energy therefore results in more ballistic photons at depth, but this approach has its limits.

In fact, it has been shown that in biological tissue the ballistic power decreases exponentially with depth as a result of scattering⁷. Consequently, as the input power is increased to counteract this effect, a new problem emerges. The beam intensity becomes high enough such that tissue at the surface of the sample — outside of the perifocal region — can fluoresce. This out-of-focus fluorescence results in undesired photons obscuring the features of interest and, once again, limits the depth at which effective imaging can be performed⁹. It is this undesired fluorescence that limited the amplified approach of Theer *et al.*¹⁶, as the features in their images became clouded at depths of around 1 mm. This loss of signal compared with the noise is not a result of limited pulse energy — only 225 nJ of the ~3 µJ available (roughly 29% of the available laser power) was used — but rather results from the out-of-focus fluorescence at the surface of the specimen. Hence, alternative strategies are now actively being pursued.

Long-wavelength excitation

One of the most effective tactics for imaging at depth exploits a key feature that made nonlinear imaging compelling in the first place: the use of longer excitation wavelengths. By moving away from 800 nm towards 1,280 nm, Kobat *et al.*^{10,47} have been able to perform *in vivo* TPEF imaging in a mouse cortex at depths as great as 1.6 mm (Fig. 4). This improvement in depth is a result of decreased scattering at the 1,280 nm wavelength generated from their Ti:sapphire pumped optical parametric oscillator. This choice of laser is significant, as it provides a high-repetition-rate (80 MHz) pulse train with modest pulse energies (~1.5 nJ), which facilitates rapid imaging. Although the use of a longer wavelength compromises the resolution slightly, the benefits of improved depth penetration⁴⁸ and facile multimodal detection^{3,49} makes the concession worthwhile for many applications.

Imaging through gradient-index lenses

The dual complications of reduced power as a function of depth and increased out-of-focus background fluorescence can be completely obviated through the use of gradient-index (GRIN) lenses. This technique was demonstrated by Levene *et al.*⁵⁰, who used needle-like (320 μ m diameter) GRIN lenses that can penetrate directly into the specimen and perform *in vivo* multiphoton imaging at depths of several millimetres. Appropriately engineered GRIN lenses effectively relay the focal plane of the microscope over tens of millimetres (even centimetre) distances, as the lens is pressed into the tissue up to the layer of interest. Using 0.6-NA GRIN lenses, Levene *et al.* achieved a circular field-of-view measuring 58 μ m in diameter and axially scanned over a distance of 95 μ m without needing to shift the GRIN lens. A natural extension of GRIN technology is to consider complete endoscopic multiphoton imaging platforms. Indeed, this is a vibrant area of development^{51–54} and features millimetre-diameter probes that are suitable for clinical applications⁵⁴.

Photo-activatable fluorophores

Other approaches for imaging at depth that are less invasive than GRIN technology include the incorporation of photo-activatable fluorophores⁵⁵, as recently demonstrated by Chen *et al.*⁵⁶. In their technique, the fluorophores remain in a dark state (that is, a non-fluorescent state) until optically triggered by multiphoton excitation. In this case, the ratio of the signal-to-background fluorescence is improved by using one multiphoton source, centred at 830 nm, to activate the fluorophores, and a second source, centred at 920 nm, to produce TPEF signal from the activated sites. This multiphoton activation strategy allows a larger number of fluorophores to be activated within the focal plane compared with the out-of-focus regions, thus resulting in a measurable increase in the signal-to-background ratio. Indeed, starting with control samples that are engineered to mimic the fundamental depth limits (where the signal-to-background ratio equals unity), Chen *et al.*⁵⁶ have demonstrated signal-to-background ratios of around 20 by using the photo-activation approach. In general, customizing probes⁵⁷ for deep imaging, as briefly discussed here, is a field in and of itself (see Extermann *et al.*⁵⁸ for an example of a deep SHG probe — a completely different approach from the one discussed here) and further elaboration is outside the scope of this Review.

Photon counting

As the imaging depth is increased, another additional complication is the scattering of the signal photons. If the signal light is collected in a non-imaging modality using single-element detection, such as with a PMT, multiple scattering events en route to the detector are not necessarily detrimental. Essentially, collecting scattered light at angles or in regions beyond the cone of light defined by the excitation beam enforces the requirement of maintaining high-NA collection over a large field-of-view; hence the drive towards high-

NA, low-magnification objectives⁵⁹. Having collected the light, it is often the case when working in this regime that there is essentially less than one signal photon generated per excitation pulse. In such a situation, it becomes beneficial to incorporate photon counting detection in order to discriminate signal photons from background noise. Until recently, this was considered prohibitive given the repetition rates of the lasers, which are in the range of 70–100 MHz. However, with the advent of inexpensive, high-performance microelectronics such as field-programmable gate arrays^{60–63}, the implementation of photon-counting circuitry is not only quite feasible, but also very economical. Driscoll *et al.*³⁵ have shown that through proper implementation of photon counting, and by accounting for the censor period of the detector, the signal-to-noise ratio can be measurably improved. This improvement is sufficient to extend photon counting for operation in the high-emission-rate regime, where analogue integration is generally thought to be required³⁵.

Adaptive optics

A final notable consideration for improving multiphoton imaging at depth is the incorporation of adaptive optical schemes. The breadth of innovation in terms of adaptive optical correction is worthy of a review in and of itself, and is therefore only briefly considered here. One of the most intriguing pathways for the implementation of adaptive optics, with respect to deep imaging, is to incorporate a system that is capable of rapidly adjusting the wavefront to accommodate aberrations induced by both the optical delivery system and the specimen without a direct assessment of the aberrated wavefront^{64–70}. Rather than assessing the wavefront directly, the image is corrected based on metrics derived from the image itself. This ‘sensorless’ approach has recently been analysed in detail by Facomprez *et al.*⁷¹, who established a useful series of guiding principles that can be employed to optimize adaptive optical strategies. Interestingly, they demonstrated that adaptive systems incorporating this philosophy are compatible with biological systems, both in terms of the speed at which corrections can be implemented and the light levels that must be used to achieve accurate correction.

High-speed imaging

Owing to the raster-scanning nature of most imaging systems in MPM and the limited number of emitted signal photons available for constructing an image, accessing dynamic behaviour in a 3D volume has proven to be an interesting challenge. Several different strategies for approaching rapid imaging are described here, but this is by no means a comprehensive list. Each of these techniques comes with its own particular strengths and weaknesses, which should be carefully weighed in order to adopt an optimal imaging approach.

Multifocal microscopy

One of the most widely used strategies for improving the frame rate in MPM is the use of multiple foci to parallelize the imaging process. Simply put, by distributing the excitation light over multiple foci, the time required to scan the focal plane is reduced accordingly. For example, when scanning linearly, two foci cover a fixed field-of-view in half the time, and subsequent gains in the frame-rate scale proportionately to the number of foci⁷². However, as the density of foci increases, the axial resolution decreases as a result of constructive interference between the foci. Fortunately, this problem can be overcome by delaying each focal spot temporally with respect to its neighbours by an amount of the order of the pulse duration (or slightly greater). In this way, the interference is entirely eliminated and the axial resolution from a 2D array of focal spots is equivalent to that of its single-focal-spot counterpart^{72–76}. Truly remarkable frame rates have been achieved through this approach. Bahlmann *et al.*⁷⁷ have successfully exceeded frame rates of 600 Hz.

In a multifocal microscope, a single-element detector can no longer be used to collect the excited photons from the sample, so it becomes necessary to use a camera⁷⁸. The necessity for a 2D detector stems from the implementation of a 2D spatial matrix of excitation foci within the sample. The emitted signal photons generated by this matrix must be imaged to their conjugate positions on the detector, as opposed to collecting all of the photons in single-element detection. If the signal photons are scattered, they will not be correctly mapped to the conjugate image position by the optical system, thus resulting in a background haze in the images. This limitation can be mitigated somewhat by introducing a segmented detector and utilizing descanned detection, in which emitted photons are detected after the scan system. Kim *et al.*⁷⁹ have successfully established this strategy. In their configuration, a multi-anode PMT is used to match the coordinates of the foci within the sample such that each anode receives the vast majority of photons emitted from a particular focus⁷⁹. This mode of operation permits the multifocal microscope to operate in a similar fashion to that of a single-focal-spot, single-element detection system. Kim *et al.* have successfully demonstrated that using 64 foci can extend the effective imaging depth from less than 30 μm to around 75 μm in neuronal tissue⁷⁹.

High-speed scan systems

Another important strategy in high-speed imaging is simply to raster the beam as fast as possible. As such, polygonal mirrors and resonant scanners hold an important place in high-speed MPM, as these systems provide a way to image 2D areas at video rates — 30 Hz (refs 80,81) — without losing the ability to explore deep within scattering tissue⁸². In such systems, practical image speeds are essentially dictated by the number of excitation pulses per pixel dwell time. With lasers operating at repetition rates of 75–100 MHz, pixel dwell times of the order of 150 ns are needed to ensure ~10 pulses per pixel. A second design consideration when optimizing the frame rate for systems scanned in this manner involves the scan's 'dead time'. For polygonal mirrors this problem occurs when the laser beam hits the interface between mirror facets and, for resonant scan mirrors, the nonlinear scan region where the mirrors are accelerating and decelerating.

Acousto-optics and tunable lenses

Although polygonal mirrors and resonant scanners can permit rapid imaging, they lack flexibility in terms of their ability to target special features of interest within the field-of-view. Acousto-optic deflectors and tunable lenses have been introduced to permit this freedom of imaging region selection, as the inertia of moving scan mirrors or the objective is no longer an issue^{83–85}. This capability allows researchers to image only the most important objects within a volume⁸⁶. Such systems can dramatically reduce the time spent imaging (allowing acquisition rates of up to 10 kHz (ref. 87)) and reduce photodamage in living specimens⁸⁸, as features that are of no interest to the research at hand are not processed with the beam. This technique has even been expanded to handle random-access imaging in three dimensions^{87,89}, thus permitting researchers to select multiple locations for imaging even when these locations are not within the same lateral plane. These systems are the result of exquisite engineering efforts that not only enable unprecedented access, but also compensate for the pulse dispersion and wavelength dependence introduced by the acousto-optic deflector^{82,90} and/or the aberrations and loss of effective NA introduced through the tunable lens^{83,91}.

Spatiotemporal focusing

An alternative strategy for improving imaging speeds and potentially simplifying MPM designs is to use an extended geometry such as a line cursor (as opposed to a point focus). The first video-rate multiphoton microscope was based on such an approach⁹². The

challenge with this method is that resolution is compromised along the low-NA dimension of the excitation source, although spatiotemporal focusing can be used to address this issue^{93,94}. Spatiotemporal focusing involves directing the laser pulse through a spectrally dispersive element, such as a prism or a diffraction grating, such that the beam is angularly dispersed as a function of wavelength. This configuration produces a situation in which the different frequencies that comprise the laser pulse are no longer overlapping spatially and, as a result, cannot add together to produce a short transform-limited pulse in time. Through the application of an appropriately designed image-relay system, these spatially separate frequencies can be made to overlap, but only at the focus of the microscope objective. Consequently, the laser pulse is transform limited only at the focal plane. The out-of-focus light pulse not only exhibits an extended spatial footprint (lowering the intensity), but is also 'stretched' in time (which also lowers the intensity). The combination of pulse focusing and defocusing, both from a spatial and a temporal point of view, causes a localization in peak intensity, such that extended source geometries can achieve an axial resolution equivalent to that of their diffraction-limited single-point counterparts^{93–98}. However, because this is a whole-field technique and therefore requires an imaging detector, it may not be well-suited to imaging at depths of more than 250 μm within scattering media⁹⁹. Even so, the ability of this technique to perform whole-field detection with tight axial sectioning is an enabling technology for many areas of research. Andrasfalvy *et al.*¹⁰⁰ have demonstrated this in their optogenetics work, in which spatiotemporal focusing permits selective control of neuronal activity at the single-cell level through two-photon activation of Channelrhodopsin-2.

Remote focusing

Finally, most high-speed imaging has focused on techniques for the rapid raster scanning of lateral images. Recent developments have led to the 'remote focusing' technique, which allows rapid axial scanning of the beam^{101,102}. This technique, when combined with a scan mirror system, permits novel access to biological systems, such as the ability to image an x - z plane or perform high-speed 3D imaging^{91,103,104}. Remote focusing operates by modifying the divergence of the beam at the back of the excitation objective, usually by imaging the objective's stop to an upstream location, where a second 'remote' objective is used in conjunction with a mirror at its focus. It is this second, remotely located objective-mirror combination that produces the necessary divergence at the excitation objective when the distance between the remote objective and mirror is adjusted. This configuration is similar to how a properly imaged scan-relay system is designed, although such a system operates on the angle at the back of the objective rather than the divergence. The ability to control the axial focus of the microscope by employing remote focusing represents a dramatic step forwards for biological imaging, as this allows biologists to examine specimens in three dimensions without moving either the object under examination or the objective used for imaging (Fig. 5)¹⁰⁵. This change in imaging paradigm is significant because moving the specimen requires expensive stages and can introduce significant problems for 'registering' real-world coordinates in individual frames with any previously captured data. Although moving the objective might be considered as an alternative to translating the specimen, such an endeavour degrades the image quality by moving away from the ideal objective position and can introduce vibrations that negatively impact the image quality.

Conclusion

The landscape of MPM has grown enormously since the initial application of TPEF microscopy by Denk *et al.*¹, and as such, no single article can truly do justice to the broad range of new technologies and novel explorations that have resulted. There are significant topics not addressed here, including pushing the resolution limits^{106–109}, spectrally resolved imaging¹¹⁰ and multiphoton light sheet microscopy¹¹¹.

The future for MPM looks bright from many perspectives. New femtosecond laser sources that operate reliably with exceptional ease are continuously being developed. In this regard, a significant new benchmark has recently been achieved: a femtosecond laser suitable for nonlinear microscopy can now be purchased at a price equivalent to that of a high-end microscope objective. Similarly, a broader class of optics are being optimized with specific application to femtosecond laser excitation and detection. These optical systems have higher throughput and are designed to deliver diffraction-limited focal spots and transform-limited pulse durations. As such, we can envision future systems that will continue to push the boundaries of imaging, further compelling studies that will connect chemical and physiological processes to structure and function, which will provide, for the first time, a comprehensive picture of organisms from the atomic to the macroscopic level.

Acknowledgments

The authors recognize the support of the National Institute of Biomedical Imaging and Bioengineering under the Bioengineering Research Partnership EB-003832. In addition, the authors thank E. Toberer for his assistance in preparing portions of this manuscript.

References

1. Denk W, Strickler JH, Webb WW. Two-photon laser scanning fluorescence microscopy. *Science*. 1990; 248:73–76. [PubMed: 2321027]
2. Peleg G, Lewis A, Linial M, Loew LM. Nonlinear optical measurement of membrane potential around single molecules at selected cellular sites. *Proc. Natl Acad. Sci. USA*. 1999; 96:6700–6704. [PubMed: 10359775]
3. Chu SW, et al. *In vivo* developmental biology study using noninvasive multi-harmonic generation microscopy. *Opt. Express*. 2003; 11:3093–3099. [PubMed: 19471431]
4. Cheng A, Gonçalves JT, Golshani P, Arisaka K, Portera-Cailliau C. Simultaneous two-photon calcium imaging at different depths with spatiotemporal multiplexing. *Nat. Methods*. 2011; 8:139–142. [PubMed: 21217749]
5. Stelzer EH, et al. Nonlinear absorption extends confocal fluorescence microscopy into the ultra-violet regime and confines the illumination volume. *Opt. Commun*. 1994; 104:223–228.
6. Chen IH, Chu SW, Sun CK, Cheng PC, Lin BL. Wavelength dependent damage in biological multi-photon confocal microscopy: A micro-spectroscopic comparison between femtosecond Ti:sapphire and Cr:forsterite laser sources. *Opt. Quant. Electron*. 2002; 34:1251–1266.
7. Helmchen F, Denk W. Deep tissue two-photon microscopy. *Nat. Methods*. 2005; 2:932–940. [PubMed: 16299478]
8. Yaroslavsky AN, et al. Optical properties of selected native and coagulated human brain tissues in vitro in the visible and near infrared spectral range. *Phys. Med. Biol*. 2002; 47:2059–2073. [PubMed: 12118601]
9. Theer P, Denk W. On the fundamental imaging-depth limit in two-photon microscopy. *J. Opt. Soc. Am. A*. 2006; 23:3139–3149.
10. Kobat D, et al. Deep tissue multiphoton microscopy using longer wavelength excitation. *Opt. Express*. 2009; 17:13354–13364. [PubMed: 19654740]
11. Ntziachristos V. Going deeper than microscopy: The optical imaging frontier in biology. *Nat. Methods*. 2010; 7:603–614. [PubMed: 20676081]
12. Barad Y, Eisenberg H, Horowitz M, Silberberg Y. Nonlinear scanning laser microscopy by third harmonic generation. *Appl. Phys. Lett*. 1997; 70:922–924.
13. Masihzadeh O, Schlup P, Bartels RA. Label-free second harmonic generation holographic microscopy of biological specimens. *Opt. Express*. 2010; 18:9840–9851. [PubMed: 20588833]
14. Zhuo S, et al. Label-free monitoring of colonic cancer progression using multiphoton microscopy. *Biomed. Opt. Express*. 2011; 2:615–619. [PubMed: 21412466]
15. Segawa H, et al. Label-free tetra-modal molecular imaging of living cells with CARS, SHG, THG and TSFG (coherent anti-Stokes Raman scattering, second harmonic generation, third harmonic

- generation and third-order sum frequency generation). *Opt. Express*. 2012; 20:9551–9557. [PubMed: 22535046]
16. Theer P, Hasan MT, Denk W. Two-photon imaging to a depth of 1000 μm in living brains by use of a $\text{Ti:Al}_2\text{O}_3$ regenerative amplifier. *Opt. Lett.* 2003; 28:1022–1024. [PubMed: 12836766]
 17. Yue S, Slipchenko M, Cheng JX. Multimodal nonlinear optical microscopy. *Las. Photon. Rev.* 2011; 5:496–512.
 18. Chung CY, Boik J, Potma EO. Biomolecular imaging with coherent nonlinear vibrational microscopy. *Ann. Rev. Phys. Chem.* 2013; 64:77–99. [PubMed: 23245525]
 19. Larson A, Yeh A. *Ex vivo* characterization of sub-10-fs pulses. *Opt. Lett.* 2006; 31:1681–1683. [PubMed: 16688260]
 20. Pestov D, Xu B, Li H, Dantus M. Delivery and characterization of sub-8fs laser pulses at the imaging plane of a two-photon microscope. *Proc. SPIE*. 2011; 7903:79033B.
 21. Selm R, Krauss G, Leitenstorfer A, Zumbusch A. Simultaneous second-harmonic generation, third-harmonic generation, and four-wave mixing microscopy with single sub-8 fs laser pulses. *Appl. Phys. Lett.* 2011; 99:181124.
 22. Zipfel W, Williams R, Webb WW. Nonlinear magic: Multiphoton microscopy in the biosciences. *Nature Biotechnol.* 2003; 21:1369–1377. [PubMed: 14595365]
 23. Mertz J. Nonlinear microscopy: New techniques and applications. *Curr. Opin. Neurobiol.* 2004; 14:610–616. [PubMed: 15464895]
 24. Svoboda K, Yasuda R. Principles of two-photon excitation microscopy and its applications to neuroscience. *Neuron*. 2006; 50:823–839. [PubMed: 16772166]
 25. Sheetz KE, Squier J. Ultrafast optics: Imaging and manipulating biological systems. *J. Appl. Phys.* 2009; 105:051101.
 26. Carriles R, et al. Invited review article: Imaging techniques for harmonic and multiphoton absorption fluorescence microscopy. *Rev. Sci. Instr.* 2009; 80:081101.
 27. Field J, et al. Optimizing the fluorescent yield in two-photon laser scanning microscopy with dispersion compensation. *Opt. Express*. 2010; 18:13661–13672. [PubMed: 20588500]
 28. Gannaway JN, Sheppard CJR. Second-harmonic imaging in the scanning optical microscope. *Opt. Quant. Electron.* 1978; 10:435–439.
 29. Raghunathan V, Han Y, Korth O, Ge NH, Potma E. Rapid vibrational imaging with sum frequency generation microscopy. *Opt. Lett.* 2011; 30:3891–3893. [PubMed: 21964132]
 30. Fu D, et al. Quantitative chemical imaging with multiplex stimulated Raman scattering microscopy. *J. Am. Chem. Soc.* 2012; 134:3623–3626. [PubMed: 22316340]
 31. Zumbusch A, Holtom GR, Xie XS. Three-dimensional vibrational imaging by coherent anti-Stokes Raman scattering. *Phys. Rev. Lett.* 1999; 82:4142–4145.
 32. Chen H, et al. A multimodal platform for nonlinear optical microscopy and microspectroscopy. *Opt. Express*. 2009; 17:1282–1290. [PubMed: 19188956]
 33. Becker, W.; Bergmann, A. Lifetime-resolved imaging in nonlinear microscopy. In: Masters, B.; So, P., editors. *Handbook of Biomedical Nonlinear Optical Microscopy*. Oxford University; 2008. p. 499–556.
 34. Becker W, et al. Fluorescence lifetime imaging by time-correlated single photon counting. *Microsc. Res. Tech.* 2004; 63:58–66. [PubMed: 14677134]
 35. Driscoll JD, et al. Photon counting, censor corrections, and lifetime imaging for improved detection in two-photon microscopy. *J. Neurophysiol.* 2011; 105:3106–3113. [PubMed: 21471395]
 36. Pastrirk I, Cruz J, Walowicz K, Lozovoy V, Dantus M. Selective two-photon microscopy with shaped femtosecond pulses. *Opt. Express*. 2003; 11:1695–1701. [PubMed: 19466048]
 37. Cruz J, Pastrirk I, Comstock M, Lozovoy V, Dantus M. Use of coherent control methods through scattering biological tissue to achieve functional imaging. *Proc. Natl Acad. Sci. USA*. 2004; 101:16996–17001. [PubMed: 15569924]
 38. Cruz J, Pastrirk I, Comstock M, Dantus M. Multiphoton intrapulse interference: Coherent control through scattering tissue. *Opt. Express*. 2004; 12:4144–4149. [PubMed: 19483957]

39. Meshulach D, Silberberg Y. Coherent quantum control of two-photon transitions by a femtosecond laser pulse. *Nature*. 1998; 396:239–242.
40. Pillai R, et al. Multiplexed two-photon microscopy of dynamic biological samples with shaped broadband pulses. *Opt. Express*. 2009; 17:12741–12752. [PubMed: 19654680]
41. Fischer M, et al. Two-photon absorption and self-phase modulation measurements with shaped femtosecond laser pulses. *Opt. Lett.* 2005; 30:1551–1553. [PubMed: 16007804]
42. Fischer M, Liu H, Piletic I, Warren W. Simultaneous self-phase modulation and two-photon absorption measurement by a spectral homodyne Z-scan method. *Opt. Express*. 2008; 16:4192–4205. [PubMed: 18542515]
43. Fischer M, et al. Self-phase modulation signatures of neuronal activity. *Opt. Lett.* 2008; 33:219–221. [PubMed: 18246134]
44. Beaurepaire E, Oheim M, Mertz J. Ultra-deep two-photon fluorescence excitation in turbid media. *Opt. Commun.* 2001; 188:25–29.
45. Ohem M, Beaurepaire E, Chaigneau E, Mertz J, Charpak S. Two-photon microscropy in brain tissue: Parameters influencing the imaging depth. *J. Neurosci. Meth.* 2001; 111:29–37.
46. Buehler C, Kim KH, Dong CY, Masters B, So PTC. Innovations in two-photon deep tissue microscopy. *Eng. Med. Biol. Mag.* 1999; 18:23–30.
47. Kobat D, Horton NG, Xu C. *In vivo* two-photon microscopy to 1.6-mm depth in mouse cortex. *J. Biomed. Opt.* 2011; 16:106014. [PubMed: 22029361]
48. Balu M, et al. Effect of excitation wavelength on penetration depth in nonlinear optical microscopy of turbid media. *J. Biomed. Opt.* 2009; 14:010508. [PubMed: 19256688]
49. Chu SW, et al. Multimodal nonlinear spectral microscopy based on a femtosecond Cr:forsterite laser. *Opt. Lett.* 2001; 26:1909–1911. [PubMed: 18059734]
50. Levene MJ, Dombeck DA, Kasischke KA, Molloy RP, Webb WW. *In vivo* multiphoton microscopy of deep brain tissue. *J. Neurophysiol.* 2004; 91:1908–1912. [PubMed: 14668300]
51. Jung W, et al. Miniaturized probe based on a microelectromechanical system mirror for multiphoton microscopy. *Opt. Lett.* 2008; 33:1324–1326. [PubMed: 18552946]
52. Chia SH, et al. Miniaturized video-rate epi-third-harmonic-generation fiber-microscope. *Opt. Express*. 2010; 18:17382–17391. [PubMed: 20721125]
53. Saar BG, Johnston RS, Freudiger CW, Xie XS, Seibel EJ. Coherent Raman scanning fiber endoscopy. *Opt. Lett.* 2011; 36:2396–2398. [PubMed: 21725423]
54. Rivera DR, Brown CM, Ouzounov DG, Webb WW, Xu C. Multifocal multiphoton endoscope. *Opt. Lett.* 2012; 37:1349–1351. [PubMed: 22513682]
55. Martini J, et al. Multifocal two-photon laser scanning microscopy combined with photo-activatable GFP for *in vivo* monitoring of intracellular protein dynamics in real time. *J. Struct. Biol.* 2007; 158:401–409. [PubMed: 17363273]
56. Chen Z, Wei L, Zhu X, Min W. Extending the fundamental imaging-depth limit of multi-photon microscopy by imaging with photo-activatable fluorophores. *Opt. Express*. 2012; 20:18525–18536. [PubMed: 23038491]
57. Cheng PC, et al. Highly efficient upconverters for multiphoton fluorescence microscopy. *J. Microsc.* 1998; 189:199–212.
58. Extermann J, et al. Nanodoublers as deep imaging markers for multi-photon microscopy. *Opt. Express*. 2009; 17:15342–15349. [PubMed: 19688012]
59. Zinter JP, Levene MJ. Maximizing fluorescence collection efficiency in multiphoton microscopy. *Opt. Express*. 2011; 19:15348–15362. [PubMed: 21934897]
60. Amir W, et al. Simultaneous imaging of multiple focal planes using a two-photon scanning microscope. *Opt. Lett.* 2007; 32:1731–1733. [PubMed: 17572762]
61. Carriles R, Sheetz KE, Hoover EE, Squier JA, Barzda V. Simultaneous multifocal, multiphoton, photon counting microscopy. *Opt. Express*. 2008; 16:10364–10371. [PubMed: 18607447]
62. Benninger RKP, Ashby WJ, Ring EA, Piston DW. Single-photon-counting detector for increased sensitivity in two-photon laser scanning microscopy. *Opt. Lett.* 2008; 33:2895–2897. [PubMed: 19079484]

63. Sandkuijl D, Cisek R, Major A, Barzda V. Differential microscopy for fluorescence-detected nonlinear absorption linear anisotropy based on a staggered two-beam femtosecond Yb:KGW oscillator. *Biomed. Opt. Express*. 2010; 1:895–901. [PubMed: 21258516]
64. Sherman L, Ye JY, Albert O, Norris TB. Adaptive correction of depth-induced aberrations in multiphoton scanning microscopy using a deformable mirror. *J. Microsc.* 2002; 206:65–71. [PubMed: 12000564]
65. Neil MAA, et al. Adaptive aberration correction in a two-photon microscope. *J. Microsc.* 2000; 200:105–108. [PubMed: 11106950]
66. Albert O, Sherman L, Mourou G, Norris TB. Smart microscope: An adaptive optics learning system for aberration correction in multiphoton confocal microscopy. *Opt. Lett.* 2000; 25:52–54. [PubMed: 18059779]
67. Booth MJ, Neil MAA, Juškaitis R, Wilson T. Adaptive aberration correction in a confocal microscope. *Proc. Natl Acad. Sci. USA*. 2002; 99:5788–5792. [PubMed: 11959908]
68. Ji N, Milkie D, Betzig E. Adaptive optics via pupil segmentation for high-resolution imaging in biological tissues. *Nat. Methods*. 2009; 7:141–147. [PubMed: 20037592]
69. Leray A, Mertz J. Rejection of two-photon fluorescence background in thick tissues by differential aberration imaging. *Opt. Express*. 2006; 14:10565–10573. [PubMed: 19529458]
70. Girkin JM, Poland S, Wright AJ. Adaptive optics for deeper imaging of biological samples. *Curr. Opin. Biotechnol.* 2009; 20:106–110. [PubMed: 19272766]
71. Facomprez A, Beaurepaire E, Débarre D. Accuracy of correction in modal sensorless adaptive optics. *Opt. Express*. 2012; 20:2598–2612. [PubMed: 22330498]
72. Bewersdorf J, Pick R, Hell SW. Multifocal multiphoton microscopy. *Opt. Lett.* 1998; 23:655–657. [PubMed: 18087301]
73. Buist AH, Müller M, Squier J, Brakenhoff GJ. Real time two-photon absorption microscopy using multi point excitation. *J. Microsc.* 1998; 192:217–226.
74. Straub M, Hell SW. Multifocal multiphoton microscopy: A fast and efficient tool for 3-D fluorescence imaging. *Bioimaging*. 1998; 6:177–185.
75. Egner A, Hell SW. Time multiplexing and parallelization in multifocal multiphoton microscopy. *J. Opt. Soc. Am. A*. 2000; 17:1192–201.
76. Nielsen T, Fricke M, Hellweg D, Andresen P. High efficiency beam splitter for multifocal multiphoton microscopy. *J. Microsc.* 2001; 201:368–376. [PubMed: 11240852]
77. Bahlmann K, et al. Multifocal multiphoton microscopy (MMM) at a frame rate beyond 600 Hz. *Opt. Express*. 2007; 15:10991–10998. [PubMed: 19547456]
78. Niesner R, Andresen V, Neumann J, Spiecker H, Gunzer M. The power of single and multibeam two-photon microscopy for high-resolution and high-speed deep tissue and intravital imaging. *Biophys. J.* 2007; 93:2519–2529. [PubMed: 17557785]
79. Kim KH, et al. Multifocal multiphoton microscopy based on multianode photomultiplier tubes. *Opt. Express*. 2007; 15:11658–11678. [PubMed: 19547526]
80. Lee AMD, et al. *In vivo* video rate multiphoton microscopy imaging of human skin. *Opt. Lett.* 2011; 36:2865–2867. [PubMed: 21808340]
81. Fan G, Fujisaki H, Miyakawa A, Tsien R, Ellisman M. Video-rate scanning two-photon excitation fluorescence microscopy and ratio imaging with chameleons. *Biophys. J.* 1999; 76:2412–2420. [PubMed: 10233058]
82. Veilleux I, Spencer JA, Biss DP, Côté D, Lin CP. *In vivo* cell tracking with video rate multimodality laser scanning microscopy. *IEEE J. Sel. Top. Quant. Electron.* 2008; 14:10–18.
83. Grewe BF, Voigt FF, van't Hoff M, Helmchen F. Fast two-layer two-photon imaging of neuronal cell populations using an electrically tunable lens. *Biomed. Opt. Express*. 2011; 2:2035–2046. [PubMed: 21750778]
84. Bullen A, Patel S, Saggau P. High-speed, random-access fluorescence microscopy: I. High-resolution optical recording with voltage-sensitive dyes and ion indicators. *Biophys. J.* 1997; 73:477–491. [PubMed: 9199810]
85. Shao Y, et al. Ultrafast, large-field multiphoton microscopy based on an acousto-optic deflector and a spatial light modulator. *Opt. Lett.* 2012; 37:2532–2534. [PubMed: 22743445]

86. Saloméa R, et al. Ultrafast random-access scanning in two-photon microscopy using acousto-optic deflectors. *J. Neurosci. Meth.* 2006; 154:161–74.
87. Reddy GD, Kelleher K, Fink R, Saggau P. Three-dimensional random access multiphoton microscopy for functional imaging of neuronal activity. *Nature Neurosci.* 2008; 11:713–720. [PubMed: 18432198]
88. Koenig K, Liang H, Berns M, Tromberg BJ. Cell damage in near-infrared multimode optical traps as a result of multiphoton absorption. *Opt. Lett.* 1996; 21:1090–1092. [PubMed: 19876262]
89. Kirkby PA, Nadella KMNS, Silver RA. A compact acousto-optic lens for 2D and 3D femtosecond based 2-photon microscopy. *Opt. Express.* 2010; 18:13721–13745. [PubMed: 20588506]
90. Kremer Y, et al. A spatio-temporally compensated acousto-optic scanner for two-photon microscopy providing large field of view. *Opt. Express.* 2008; 16:10066–10076. [PubMed: 18607414]
91. Botcherby EJ, et al. Aberration-free three-dimensional multiphoton imaging of neuronal activity at kHz rates. *Proc. Natl Acad. Sci. USA.* 2012; 109:2919–2924. [PubMed: 22315405]
92. Brakenhoff GJ, et al. Real-time two-photon confocal microscopy using a femtosecond, amplified Ti:sapphire system. *J. Microsc.* 1996; 181:253–259. [PubMed: 8642584]
93. Oron D, Tal E, Silberberg Y. Scanningless depth-resolved microscopy. *Opt. Express.* 2005; 13:1468–1476. [PubMed: 19495022]
94. Zhu G, van Howe J, Durst M, Zipfel WR, Xu C. Simultaneous spatial and temporal focusing of femtosecond pulses. *Opt. Express.* 2005; 13:2153–2159. [PubMed: 19495103]
95. Therrien OD, Aubé B, Pagès S, De Koninck P, Côté D. Wide-field multiphoton imaging of cellular dynamics in thick tissue by temporal focusing and patterned illumination. *Biomed. Opt. Express.* 2011; 2:696–704. [PubMed: 21412473]
96. Cheng LC, et al. Spatiotemporal focusing-based widefield multiphoton microscopy for fast optical sectioning. *Opt. Express.* 2012; 20:8939–8948. [PubMed: 22513605]
97. Durst ME, Zhu G, Xu C. Simultaneous spatial and temporal focusing in nonlinear microscopy. *Opt. Commun.* 2008; 281:1796–1805. [PubMed: 18496597]
98. Durst ME, Straub AA, Xu C. Enhanced axial confinement of sum-frequency generation in a temporal focusing setup. *Opt. Lett.* 2009; 34:1786–1788. [PubMed: 19529703]
99. Mohanty SK, et al. In-depth activation of channelrhodopsin 2-sensitized excitable cells with high spatial resolution using two-photon excitation with a near-infrared laser microbeam. *Biophys. J.* 2008; 95:3916–3926. [PubMed: 18621808]
100. Andrasfalvy BK, Zemelman BV, Tang J, Vaziri A. Two-photon single-cell optogenetic control of neuronal activity by sculpted light. *Proc. Natl Acad. Sci. USA.* 2010; 107:11981–11986. [PubMed: 20543137]
101. Botcherby EJ, Booth MJ, Juškaitis R, Wilson T. Real-time extended depth of field microscopy. *Opt. Express.* 2008; 16:21843–21848. [PubMed: 19104617]
102. Botcherby EJ, Booth MJ, Juškaitis R, Wilson T. Real-time slit scanning microscopy in the meridional plane. *Opt. Lett.* 2009; 34:1504–1506. [PubMed: 19448802]
103. Hoover EE, et al. Remote focusing for programmable multi-layer differential multiphoton microscopy. *Biomed. Opt. Express.* 2010; 2:113–122. [PubMed: 21326641]
104. Anselmi F, Ventalon C, Bègue A, Ogden D, Emiliani V. Three-dimensional imaging and photostimulation by remote-focusing and holographic light patterning. *Proc. Natl Acad. Sci. USA.* 2011; 108:19504–19509. [PubMed: 22074779]
105. Hoover EE, et al. Eliminating the scattering ambiguity in multifocal, multimodal, multiphoton imaging systems. *J. Biophoton.* 2012; 5:425–436.
106. Hell SW, Wichmann J. Breaking the diffraction resolution limit by stimulated emission: Stimulated emission depletion fluorescence microscopy. *Opt. Lett.* 1994; 19:780–782. [PubMed: 19844443]
107. Betzig E, et al. Imaging intracellular fluorescent proteins at nanometer resolution. *Science.* 2006; 313:1642–1645. [PubMed: 16902090]
108. Huang B, Wenqin W, Zhuang X. Three-dimensional super-resolution imaging by stochastic optical reconstruction microscopy. *Science.* 2008; 319:810–813. [PubMed: 18174397]

109. Hell SW, Schmidt R, Egner A. Diffraction-unlimited three-dimensional optical nanoscopy with opposing lenses. *Nature Photon.* 2009; 3:381–387.
110. Wachsmann-Hogiu, S.; Farkas, DL. *Handbook of Biomedical Nonlinear Optical Microscopy.* Oxford University; 2008. Nonlinear multispectral optical imaging microscopy: Concepts, instrumentation, and applications; p. 461-480.
111. Truong T, Supatto W, Koos D, Choi J, Fraser S. Deep and fast live imaging with two-photon scanned light-sheet microscopy. *Nat. Methods.* 2011; 8:757–760. [PubMed: 21765409]

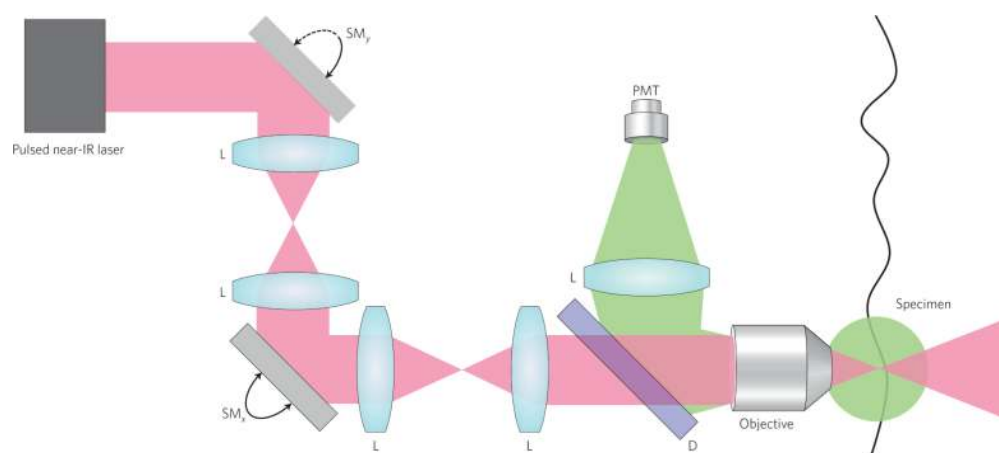


Figure 1. A typical multiphoton microscope fed by a near-IR laser

Typical multiphoton systems utilize near-IR (700–1,300 nm) light and use a raster scanning system to control the beam, either with ‘close coupled’ scan mirrors or with image-relayed scan mirrors (SM_x and SM_y, as shown here). In this epi-detection configuration, a dichroic (D) is used to separate two-photon excited fluorescence from the excitation light and direct this fluorescence to a PMT. L = lens.

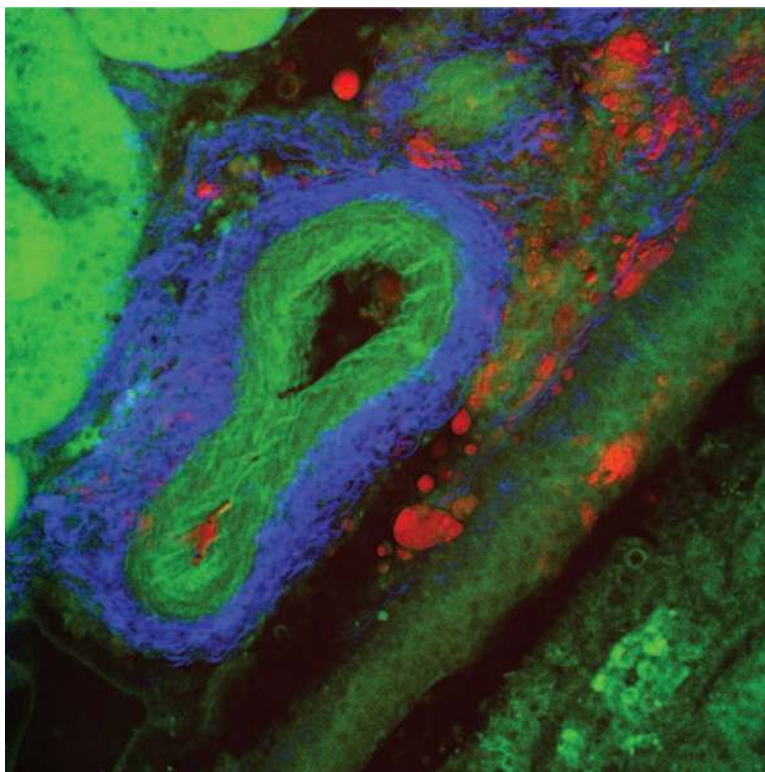


Figure 2. Multimodal image of a blood vessel in kidney tissue
SHG (blue), TPEF (green) and coherent anti-Stokes Raman scattering (red). Image courtesy of Eric Potma, University of California, Irvine, USA.

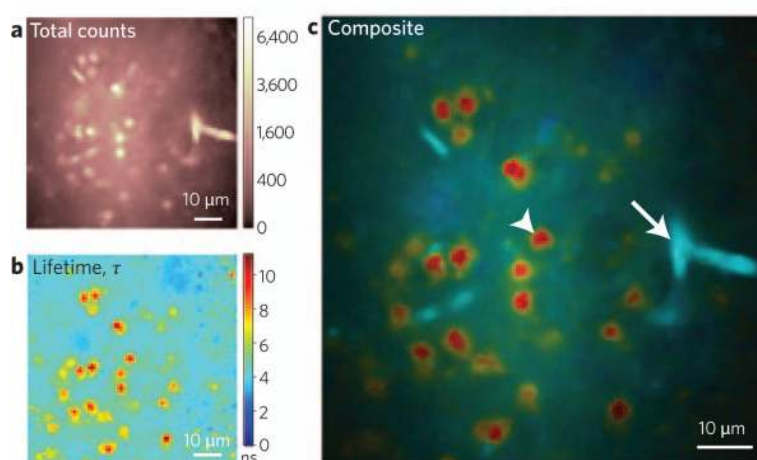


Figure 3. Illustrative fluorescence lifetime image with two similar fluorophores and comparison to TPEF imaging

Fluorescence intensity and lifetime imaging of propidium iodide (PI)-labelled cells and Texas Red dextran (TR)-labelled vessels in a mouse model. **a**, TPEF image shows that the two dyes are indistinguishable. Scale bar (right) represents photon counts. **b**, Image is rescaled according to the measured fluorescent lifetime; the PI-label and the TR-label are now spatially distinct. Scale bar (right) is in nanoseconds. **c**, The images in **a** and **b** are combined, thus enabling facile detection of the two fluorophores. The arrowhead points to a PI-labelled cell, whereas the arrow points to a TR-labelled vessel. Figure reproduced with permission from ref. 35, © 2011 APS.

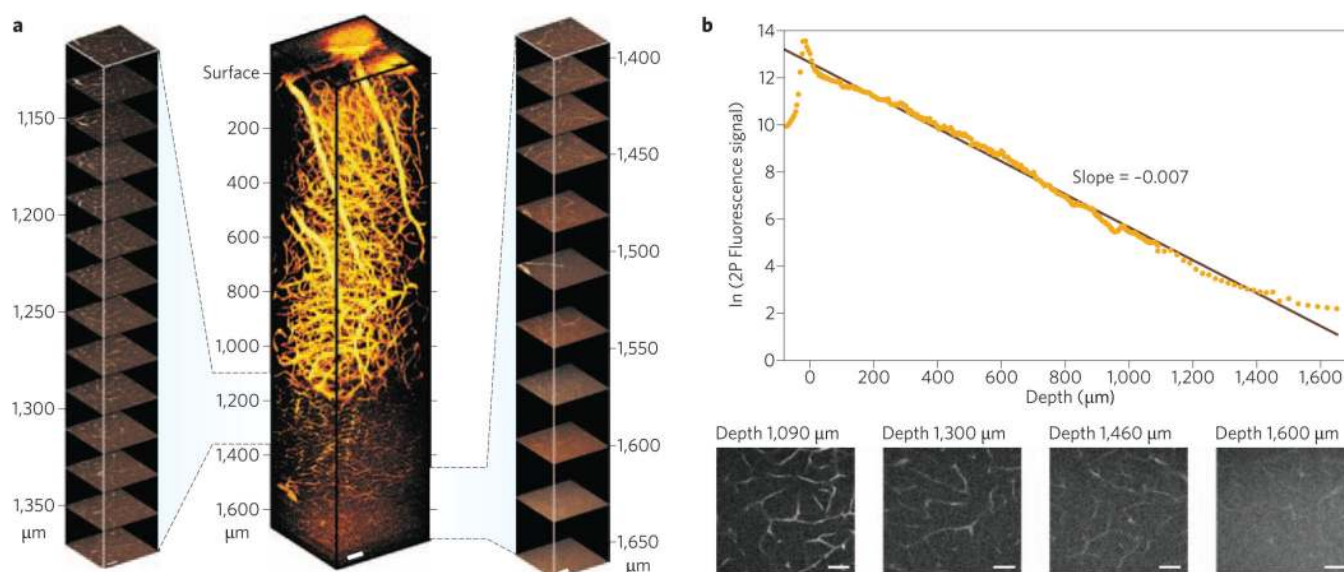


Figure 4. Example of deep *in vivo* imaging through the use of longer excitation wavelengths 1,280 nm light from an optical parametric oscillator is used to perform TPEF imaging of mouse vasculature labelled with Alexa680-Dextran. **a**, *In vivo* two-photon fluorescence images of cortical vasculature in mouse brain. 235 x - y frames from 60 μm above the cortical surface to 1,110 μm below are taken at depth increments of 5 μm . The depth increments in the stack are 20 μm in the range of 1,110–1,490 μm and 30 μm in the range of 1,490–1,670 μm . 3D reconstruction is made in Image J software using the volume viewer plug-in. Expanded 3D stacks are shown for the deepest sections ($>1,130 \mu\text{m}$). **b**, Fluorescence intensity as a function of imaging depth for the stack shown in **a**. Fluorescence signal strength at a particular depth is represented by the average value of the brightest 1% of the pixels in the x - y image at that depth. Scale bars are 50 μm for both **a** and **b**. Figure reproduced with permission from ref. 47, © 2011 SPIE.

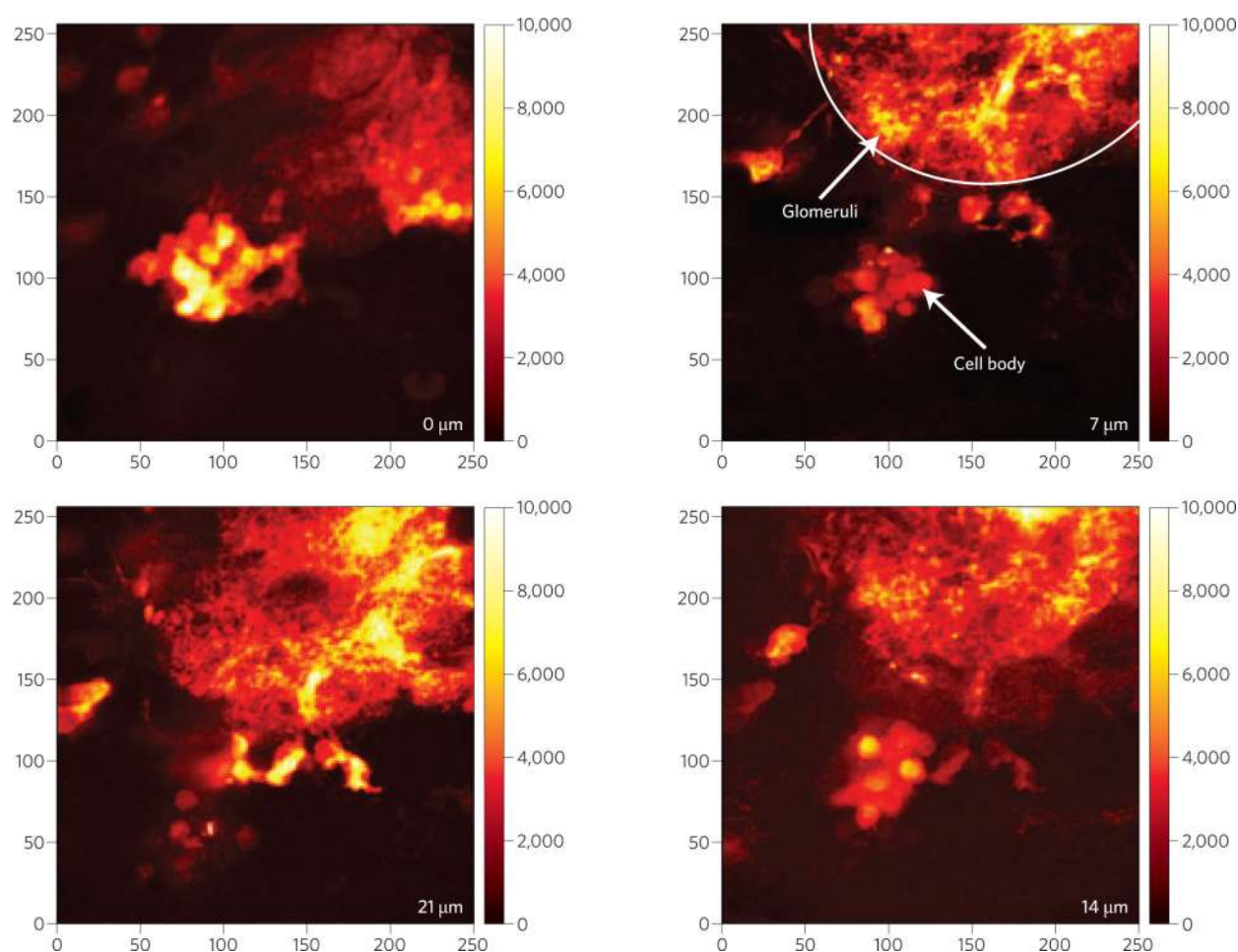


Figure 5. Simultaneous multilayer imaging achieved with remote focusing

Four images of *Drosophila melanogaster* antennal lobe structure labelled with red fluorescent protein. The images are separated axially by 7 μm in depth and were all acquired simultaneously from a single-element detector. Figure reproduced with permission from ref. 105, © 2012 Wiley.